Received <day> <Month>, <year>; | Revised <day> <Month>, <year>; | Accepted <day> <Month>, <year>

DOI: xxx/xxxx

ARTICLE TYPE

Bifurcation and comparison of a discrete-time Hindmarsh-Rose model

Yue Li*[1] | Hongjun Cao[2]

[1]Department of Mathematics, School of Science, Beijing Jiaotong University, Beijing, China
[2]Department of Mathematics, School of Science, Beijing Jiaotong University, Beijing, China

Correspondence
*Hongjun Cao, Department of Mathematics, School of Science,
Beijing Jiaotong University, Beijing 100044, P. R. China. Email: hjcao@bjtu.edu.cn

Present Address
Department of Mathematics, School of Science,
Beijing Jiaotong University, Beijing 100044, P. R. China

Abstract

In this paper, a discrete-time Hindmarsh-Rose model is obtained by a nonstandard finite difference (NSFD) scheme. Bifurcation behaviors between the model obtained by the forward Euler scheme and the model obtained by the NSFD scheme are compared. Through analytical and numerical comparisons, much more bifurcations and dynamical behaviors can be obtained and preserved by using the NSFD scheme, in which the integral step size can be chosen larger relatively due to its better stability and convergence than those in the forward Euler scheme. It means that the discrete-time model obtained by the NSFD scheme is closer to the original continuous system than the discrete-time model obtained by the forward Euler scheme. These confirmed results can at least guarantee true available numerical results to investigate complex neuron dynamical systems.

KEYWORDS:
discrete-time Hindmarsh-Rose model, nonstandard finite difference scheme, stability, fold bifurcation, Neimark-Sacker bifurcation

1 | INTRODUCTION

Many dynamical systems are represented by nonlinear differential equations whose analytical solutions are usually hard to obtain. Under this circumstance, how to take into account the dynamical behaviors of these nonlinear differential equations effectively is of great significance.

Among so many methods to deal with the above problem, the discretization is a straightforward way. There are several ways to transform a continuous differential system into a corresponding discrete mapping. The most commonly used method for this aim is the standard difference methods, such as the forward Euler scheme, the Runge-Kutta method and so on. Nevertheless, there have been so many unclear questions so far, the key point is how to preserve the basic structure and the main properties of the original continuous dynamical system after discretization as much as possible. In particular, the numerical instabilities should be considered before the implementation of standard finite difference schemes.

In order to eliminate numerical instabilities, the NSFD schemes have been proposed by many researchers, for example like[1] and therein. In general, the NSFD scheme is based on a basic rule, that is to maintain the dynamic characteristics and basic structures of the corresponding continuous model as much as possible, such as equilibria, stability of steady-states, bifurcations, and even chaos.

The main advantage of NSFD schemes is able to retain the considerable properties of their original continuous systems in order to guarantee true numerical results. While the construction of these NSFD schemes is not easy, and this is because there is no general criterion for construction. In addition, the so-called dynamically consistent problem must be considered. A discrete-time model is said to be dynamically consistent with its continuous system if both systems demonstrate the similar dynamical behaviors, such as stability behavior of steady-states, bifurcation, chaos and so on[2].

Over the past decades, there have been numerous interesting results by using the NSFD method. For example, in[3], authors developed positive and elementary stable nonstandard (PESN) finite-difference methods for predator-prey systems. They found that the PESN methods keep both the positivity of the solutions and the stability of the equilibria of the corresponding predator-prey system. A NSFD scheme which was constructed to simulate a predator-prey model of Gause-type with a functional response is consistent with the asymptotic dynamics of the model. It was also compared with those obtained from the standard methods such as the forward Euler and the Runge-Kutta methods[4]. Mickens's method was generalized by Roeger. Simultaneously, a class of nonstandard symplectic numerical methods for a Lotka-Volterra system were given[5]. Roeger et al. constructed a discrete Lotka-Volterra competition model by applying the NSFD schemes, and proved the dynamic consistency between the resulting difference equation and the differential equation[6]. Kahan et al. presented an unconventional method with the second-order accuracy[7]. Roeger used conformal mappings to study the relationship between the eigenvalues of the Jacobian matrices of the differential equations and the resulting difference equations, and proved that Kahan's discretization method preserves the local stability and the Hopf bifurcation of any fixed points while Euler's method fails. Unfortunately, Kahan's method can only be applied to the differential equation $\frac{dx}{dt} = f(x)$ where $f(x)$ is with at most quadratic in x[8]. Other applications of the NSFD scheme can be found in[9,10,11,12].

It is worth to consider whether the NSFD method is only suitable for the discretization of predator-prey model, or it can also able to discretize neuron models, such as one of the classical neuron model, Hindmarsh-Rose model. To the best of our knowledge, few NSFD schemes for Hindmarsh-Rose models have not been studied.

Many researchers have used bifurcation theory to study the complex dynamics of Hindmarsh-Rose model. In general, there are two main research directions. One is to directly make an analysis for a class of continuous Hindmarsh-Rose model. In[13], the authors proposed two Hindmarsh-Rose neurons with the same synaptic coupling and discussed how coupling strength and time delay affect dynamics by studying the stabilities and bifurcations at equilibria. Some conclusions could be regarded as the theoretical guidance for the study of dynamics of coupled neurons. The other is the discretization for continuous Hindmarsh-Rose models by using a suitable discrete format, and then to investigate the corresponding discrete-time dynamics of the Hindmarsh-Rose model. Usually, after different discrete schemes such as the forward Euler format, the fourth-order Runge-Kutta format are adopted, numerical simulations are able to explore the potential dynamics in the discrete-time Hindmarsh-Rose model.

The forward Euler scheme is the more frequently used method to discretize a Hindmarsh-Rose models. Yu and Cao[14] discretized a three-dimensional Hindmarsh-Rose model by the forward Euler scheme and then investigated the existence of one-parameter bifurcations in the discrete model. They illustrated the correctness of the bifurcation analysis by numerical computation. Li and He[15] proved that a two-dimensional discrete Hindmarsh-Rose model can produce two kinds of codimension-one bifurcations (flip bifurcation, Neimark-Sacker bifurcation) and a codimension-two bifurcation (1:1 resonance). In addition, they also carried out numerical computations, which illustrated the theoretical results and showed some complex dynamic behaviors. Felicio and Rech[16] presented a two-dimensional parameter-plane diagram for a three-dimensional discrete Hindmarsh-Rose model. Moreover, periodic structures can be observed clearly in a two-dimensional parameter-plane diagram. Kuznetsov and Sedova[17] analyzed the quasi-periodic bifurcations of a map by observing two-dimensional parameter-plane diagrams corresponding to different integral step sizes. Most of studies focuses on the discrete-time models discretized by the forward Euler scheme[18,19,20,21].

Herein, we will focus on the following modified Hindmarsh-Rose model in[22]:

$$\begin{cases} \dfrac{dx}{dt} = c\left(x - \frac{x^3}{3} - y + I\right), \\ \dfrac{dy}{dt} = \frac{x^2+dx-by+a}{c}, \end{cases} \tag{1}$$

where x represents the membrane potential, y is an internal, or recovery variable, I is the stimulus intensity, and a, b, c and d are all positive parameters. Stability and bifurcation structures of this model involving one-parameter bifurcations and the bifurcations of codimension-two were studied[22]. Li and He[23] studied the dynamic properties like periodic structures and bifurcation types of the model which is obtained by applying the forward Euler scheme to discretize model (1):

$$\begin{pmatrix} x \\ y \end{pmatrix} \mapsto \begin{pmatrix} x + \delta c\left(x - \frac{x^3}{3} - y + I\right) \\ y + \frac{\delta}{c}\left(x^2 + dx - by + a\right) \end{pmatrix}. \tag{2}$$

In this paper, a NSFD scheme is applied to model (1). One of novelties of this paper is that unlike most implicit discrete schemes which cannot be solved explicitly, the explicit expressions can be solved in this paper as equation (3), which facilitates our research. The goal is to compare the difference between the model obtained by the forward Euler scheme and the discrete-time Hindmarsh-Rose model obtained by the NSFD scheme. For the sake of simplicity in the computation, the projection method is used to calculate the normal forms of one-parameter bifurcations at the fixed points of model (3). Based on the bifurcation analysis, several behaviors for the two dimensional Hindmarsh-Rose model are simulated and compared near bifurcation points. When the step size h is the same, bifurcation parameter of the Hopf bifurcation of the model (3) which obtained by the NSFD method is closer to the original continuous model than model (2) which obtained by the forward Euler method. In addition, because of the better stability and convergence of the NSFD method, when the step size increases, the difference equation still converges, and more dynamic phenomena can be obtained such as the chaotic attractor, which is demonstrated by numerical simulation.

The layout of this paper is as follows. In section 2, from the point of view of qualitative and quantitative analysis for bifurcation, the existence and stability of the fixed points for model (3) are concerned, which makes the bifurcation analysis more accurate and the corresponding comparison more specific, especially in numerical simulation. In section 3, sufficient conditions for fold bifurcation and Neimark-Sacker bifurcation at fixed points of model (3) are given and the differences on bifurcations between model (2) and model (3) are discussed. The theoretical results are identified by numerical simulation in section 4, where complex dynamics like periodic structures, invariant closed orbits and chaotic attractor are observed. Moreover, the results of numerical simulation of the forward Euler scheme and the NSFD scheme are compared especially in two-dimensional parameter-plane diagrams. Finally, conclusions are given in section 5.

2 | EXISTENCE AND STABILITY OF FIXED POINTS OF MODEL (3)

Applying the NSFD scheme to model (1),

$$\begin{cases} \frac{X-x}{h} = \frac{c(x+X)}{2} - \frac{cx^2X}{3} - \frac{c(y+Y)}{2}, \\ \frac{Y-y}{h} = \frac{xX+\frac{d(x+X)}{2}-\frac{b(y+Y)}{2}+a}{c}, \end{cases}$$

where $h > 0$ is the step size and the approximations $x \mapsto \frac{x+X}{2}$, $x^2 \mapsto xX$, $x^3 \mapsto x^2X$ and $y \mapsto \frac{y+Y}{2}$ are used to approximate x, x^2, x^3 and y terms.

Notice that the NSFD scheme applied in this paper is an implicit method and the explicit expressions can be solved. So the following discrete-time model is obtained

$$\begin{pmatrix} x \\ y \end{pmatrix} \mapsto \begin{pmatrix} \dfrac{6h(x-2y)c^2+\big(((3b-3d)x-6a)h^2+12x\big)c+6bhx}{\big(4x^2-6\big)hc^2+\big(12+\big(2bx^2-3b+3d+6x\big)h^2\big)c+6bh} \\ \dfrac{4ch^2(\frac{dx^3}{2}+(a+\frac{3}{2}-\frac{by}{2})x^2-\frac{3xy}{2}+\frac{3}{4}y(b-d)-\frac{3a}{2})+((4x^2y-6y)c^2-6by+12(dx+x^2+a))h+12cy}{2\Big(bx^2-\frac{3}{2}b+\frac{3}{2}d+3x\Big)ch^2+\big(\big(4x^2-6\big)c^2+6b\big)h+12c} \end{pmatrix}. \tag{3}$$

As usual, assume that $I = 0$ in this paper.

In order to guarantee the model meaningful, the following conditions are assumed:

$$\begin{gathered} \left(4x^2-6\right)hc^2+\left(12+\left(2bx^2-3b+3d+6x\right)h^2\right)c+6bh \neq 0, \\ 2\left(bx^2-\frac{3}{2}b+\frac{3}{2}d+3x\right)ch^2+\left(\left(4x^2-6\right)c^2+6b\right)h+12c \neq 0. \end{gathered} \tag{4}$$

Next, the existence and stability of the fixed points of model (3) are analyzed, which provides a precondition for the analysis and comparison of the bifurcation and facilitates the selection of parameters in numerical simulation.

2.1 | Existence

The fixed points $E(x, y)$ of model (3) satisfy the following equations

$$\begin{cases} \dfrac{6h(x-2y)c^2+\big(((3b-3d)x-6a)h^2+12x\big)c+6bhx}{\big(4x^2-6\big)hc^2+\big(12+\big(2bx^2-3b+3d+6x\big)h^2\big)c+6bh} = x, \\ \dfrac{4ch^2(\frac{dx^3}{2}+(a+\frac{3}{2}-\frac{by}{2})x^2-\frac{3xy}{2}+\frac{3}{4}y(b-d)-\frac{3a}{2})+((4x^2y-6y)c^2-6by+12(dx+x^2+a))h+12cy}{2\Big(bx^2-\frac{3}{2}b+\frac{3}{2}d+3x\Big)ch^2+\big(\big(4x^2-6\big)c^2+6b\big)h+12c} = y. \end{cases} \tag{5}$$

then we have

$$\begin{cases} -\frac{6hc((\frac{bx^3}{3}+x^2+(d-b)x+a)h+\frac{2c}{3}(x^3-3x+3y))}{2ch^2(bx^2-\frac{3}{2}b+\frac{3}{2}d+3x)+((4x^2-6)c^2+6b)h+12c}=0, \\ \frac{4h(ch(\frac{dx^3}{2}+(-by+a+\frac{3}{2})x^2-3xy+\frac{3by}{2}-\frac{3dy}{2}-\frac{3a}{2})-3by+3dx+3x^2+3a)}{2ch^2(bx^2-\frac{3}{2}b+\frac{3}{2}d+3x)+((4x^2-6)c^2+6b)h+12c}=0. \end{cases} \tag{6}$$

Through variable transformations, we get the following conditions for the fixed points of model (3),

$$F(x)=\frac{b}{3}x^3+x^2+(d-b)x+a \tag{7}$$

and

$$y=x-\frac{x^3}{3}. \tag{8}$$

It is easy to find that the fixed points of model (3) are the same as the equilibria of model (1).

The number of the fixed points of the discrete model (3) is the same as model (1) which is given by[22].

2.2 | Stability

The Jacobian matrix $J(x_k, y_k)$ of model (3) evaluated at one of the above fixed points at $E_k(x_k, y_k)$ is given by

$$J\left(x_k, y_k\right)=\begin{pmatrix} J_{11} & J_{12} \\ J_{21} & J_{22} \end{pmatrix}, \tag{9}$$

where the expression of J_{11}, J_{12}, J_{21}, J_{22} are given in the Appendix.

The corresponding characteristic equation can be written as

$$h(\lambda)=\lambda^2-(Ba+C)\lambda+(Da+E)=0. \tag{10}$$

It is easy to obtain the eigenvalue

$$\lambda_{1,2}=\frac{Ba+C}{2}\pm\frac{\sqrt{\Delta}}{2},$$

where $\Delta=(Ba+C)^2-4(Da+E)$, and the the expression of B, C, D, E are presented in the Appendix.

Theorem 2.1

(i) The fixed point E_k of model (3) is a stable focus if one of the following conditions holds:

(a) $\frac{-BC+2D-2\sqrt{B^2E-BCD+D^2}}{B^2}<a<\frac{-BC+2D+2\sqrt{B^2E-BCD+D^2}}{B^2}$, $a<\frac{1-E}{D}(D>0)$;

(b) $\frac{-BC+2D-2\sqrt{B^2E-BCD+D^2}}{B^2}<a<\frac{-BC+2D+2\sqrt{B^2E-BCD+D^2}}{B^2}$, $a>\frac{1-E}{D}(D<0)$.

(ii) The fixed point E_k of model (3) is an unstable focus if one of the following conditions satisfies:

(a) $\frac{-BC+2D-2\sqrt{B^2E-BCD+D^2}}{B^2}<a<\frac{-BC+2D+2\sqrt{B^2E-BCD+D^2}}{B^2}$, $a>\frac{1-E}{D}(D>0)$;

(b) $\frac{-BC+2D-2\sqrt{B^2E-BCD+D^2}}{B^2}<a<\frac{-BC+2D+2\sqrt{B^2E-BCD+D^2}}{B^2}$, $a<\frac{1-E}{D}(D<0)$.

Theorem 2.2

(i) The fixed point E_k of model (3) is an unstable sink if one of the following conditions holds:

(a) $-a\geq\frac{2D-BC+2\sqrt{B^2E-BCD+D^2}}{B^2}$ or $a\leq\frac{2D-BC-2\sqrt{B^2E-BCD+D^2}}{B^2}$, $a<\frac{1+E-C}{B-D}(B-D<0)$, $a<\frac{-1-E-C}{B+D}(B+D>0)$;

(b) $-a\geq\frac{2D-BC+2\sqrt{B^2E-BCD+D^2}}{B^2}$ or $a\leq\frac{2D-BC-2\sqrt{B^2E-BCD+D^2}}{B^2}$, $a<\frac{1+E-C}{B-D}(B-D<0)$, $a>\frac{-1-E-C}{B+D}(B+D<0)$;

(c) $-a\geq\frac{2D-BC+2\sqrt{B^2E-BCD+D^2}}{B^2}$ or $a\leq\frac{2D-BC-2\sqrt{B^2E-BCD+D^2}}{B^2}$, $a>\frac{1+E-C}{B-D}(B-D>0)$, $a<\frac{-1-E-C}{B+D}(B+D>0)$;

(d) $-a\geq\frac{2D-BC+2\sqrt{B^2E-BCD+D^2}}{B^2}$ or $a\leq\frac{2D-BC-2\sqrt{B^2E-BCD+D^2}}{B^2}$, $a>\frac{1+E-C}{B-D}(B-D>0)$, $a>\frac{-1-E-C}{B+D}(B+D<0)$;

(e) $-a\geq\frac{2D-BC+2\sqrt{B^2E-BCD+D^2}}{B^2}$ or $a\leq\frac{2D-BC-2\sqrt{B^2E-BCD+D^2}}{B^2}$, $a<-\frac{C+2}{B}(B>0)$, $a<\frac{-1-E-C}{B+D}(B+D<0)$;

(f) $-a\geq\frac{2D-BC+2\sqrt{B^2E-BCD+D^2}}{B^2}$ or $a\leq\frac{2D-BC-2\sqrt{B^2E-BCD+D^2}}{B^2}$, $a<-\frac{C+2}{B}(B>0)$, $a>\frac{-1-E-C}{B+D}(B+D>0)$;

(g) $-a\geq\frac{2D-BC+2\sqrt{B^2E-BCD+D^2}}{B^2}$ or $a\leq\frac{2D-BC-2\sqrt{B^2E-BCD+D^2}}{B^2}$, $a>-\frac{C+2}{B}(B<0)$, $a<\frac{-1-E-C}{B+D}(B+D<0)$;

(h) $-a\geq\frac{2D-BC+2\sqrt{B^2E-BCD+D^2}}{B^2}$ or $a\leq\frac{2D-BC-2\sqrt{B^2E-BCD+D^2}}{B^2}$, $a>-\frac{C+2}{B}(B<0)$, $a>\frac{-1-E-C}{B+D}(B+D>0)$;

(i) $-a\geq\frac{2D-BC+2\sqrt{B^2E-BCD+D^2}}{B^2}$ or $a\leq\frac{2D-BC-2\sqrt{B^2E-BCD+D^2}}{B^2}$, $a>\frac{-C+2}{B}(B>0)$, $a<\frac{1+E-C}{B-D}(B-D>0)$;

(j) $-a\geq\frac{2D-BC+2\sqrt{B^2E-BCD+D^2}}{B^2}$ or $a\leq\frac{2D-BC-2\sqrt{B^2E-BCD+D^2}}{B^2}$, $a>\frac{-C+2}{B}(B>0)$, $a>\frac{1+E-C}{B-D}(B-D<0)$;

(k) $-a\geq\frac{2D-BC+2\sqrt{B^2E-BCD+D^2}}{B^2}$ or $a\leq\frac{2D-BC-2\sqrt{B^2E-BCD+D^2}}{B^2}$, $a>\frac{-C+2}{B}(B<0)$, $a<\frac{1+E-C}{B-D}(B-D>0)$;

(I) $-a \geq \frac{2D-BC+2\sqrt{B^2E-BCD+D^2}}{B^2}$ or $a \leq \frac{2D-BC-2\sqrt{B^2E-BCD+D^2}}{B^2}$, $a > \frac{-C+2}{B}(B<0)$, $a > \frac{1+E-C}{B-D}(B-D<0)$.

(ii) When $a \geq \frac{2D-BC+2\sqrt{B^2E-BCD+D^2}}{B^2}$ or $a \leq \frac{2D-BC-2\sqrt{B^2E-BCD+D^2}}{B^2}(D^2-B^2<0)$, the fixed point E_k of model (3) is a saddle.

The proof of the above two theorems is presented in the Appendix.

3 | ANALYSIS OF BIFURCATION

This section mainly focus on the one-parameter bifurcations of model (3) which is investigated by the projection method[24]. More importantly, the comparison of bifurcations between model (2) and model (3) is discussed.

Let $u = x - x_k$ and $v = y - y_k$, then we transform $E_k(x_k, y_k)$ to the origin. By introducing a new variable $X = (u, v)^T$, model (3) can be transformed in the form

$$X \mapsto G(X), \tag{11}$$

where $G = (G_1, G_2)^T$ with

$$G_1 = \frac{6hc^2(u-2v-x_k+2y_k)+((3(b-d)(u-x_k)-6a)h^2+12(u-x_k))c+6bh(u-x_k)}{4hc^2(u^2-2ux_k+x_k^2-\frac{3}{2})+(12+(2bu^2+(6-4bx_k)u+2bx_k^2+3(d-b)-6x_k)h^2)c+6bh},$$

$$\begin{aligned}G_2 = &\frac{4ch^2(\frac{du^3+(b(y_k-v)-3dx_k+3+2a)u^2}{2}+(\frac{3dx_k^2}{2}+(b(v-y_k)-2a-3)x_k+\frac{3(y_k-v)}{2})u)}{4hc^2(u^2-2ux_k+x_k^2-\frac{3}{2})+\left(12+((2u^2-4ux_k+2x_k^2-3)b+3d+6u-6x_k)h^2\right)c+6bh}\\ &-\frac{ch^2(2dx_k^3+2x_k^2(b(y_k-v)+3)+6x_k\left(v-y_k\right)3v(b-d)+3y_k(d-b)-6a)}{4hc^2(u^2-2ux_k+x_k^2-\frac{3}{2})+\left(12+((2u^2-4ux_k+2x_k^2-3)b+3d+6u-6x_k)h^2\right)c+6bh}\\ &+\frac{4((4(v-y_k)(u^2-2ux_k+{x_k}^2-\frac{3}{2})c^2+12(u^2+(d-2x_k)u)+6b(y_k-v)+12({x_k}^2-dx_k+a))h+12c(v-y_k))}{4hc^2(u^2-2ux_k+{x_k}^2-\frac{3}{2})+\left(12+((2u^2-4ux_k+2{x_k}^2-3)b+3d+6u-6x_k)h^2\right)c+6bh}.\end{aligned}$$

For the model (11), we obtain

$$X \mapsto JX + \frac{1}{2}B(X,X) + \frac{1}{6}C(X,X,X) + O(|X|^4), \tag{12}$$

where $J = J(E_k)$ and $B(X,X)$ and $C(X,X,X)$ are mulitilinear functions with

$$B(x,y) = \sum_{j,k=1}^{2} \left.\frac{\partial^2 F(\xi,\delta)}{\partial \xi_j \partial \xi_k}\right|_{\xi=0} x_j y_k = \begin{pmatrix} b_1 \\ b_2 \end{pmatrix} x_1 y_1 + \begin{pmatrix} b_3 \\ b_4 \end{pmatrix} (x_1 y_2 + x_2 y_1),$$

and

$$\begin{aligned}C(x,y,w) &= \sum_{2}^{j,k,l=1} \left.\frac{\partial^3 F(\xi,\delta)}{\partial \xi_j \partial \xi_k \partial \xi_l}\right|_{\xi=0} x_j y_k w_l \\ &= \begin{pmatrix} c_1 \\ c_2 \end{pmatrix} x_1 y_1 w_1 + \begin{pmatrix} c_3 \\ c_4 \end{pmatrix} \left(x_1 y_1 w_2 + x_1 y_2 w_1 + x_2 y_1 w_1\right)\end{aligned}$$

where the expression of b_1, b_2, b_3, b_4 and c_1, c_2, c_3, c_4 are given in the Appendix.

3.1 | Fold bifurcation

In the following analysis of the fold bifurcation, the parameter a is chosen as the bifurcation parameter. Bifurcation analysis for the model (1)-(3) is performed by the bifurcation theory at $E_k(x_k, y_k)$, which is more convenient to make a comparison of bifurcation between these three models.

First, the characteristic polynomial corresponding to the Jacobian matrix at the fixed point $E_k(x_k, y_k)$ of model (1) is

$$H(\lambda) = \lambda^2 - \left(-cx_k^2 + c - \frac{b}{c}\right)\lambda + bx_k^2 + 2x_k - b + d.$$

A fold bifurcation may occur at the fixed point $E_k(x_k, y_k)$ if the following conditions are satisfied[24]:

$$\begin{cases} H(0) = bx_k^2 + 2x_k - b + d = 0, \\ \frac{b}{3}x_k^3 + x_k^2 + (d-b)x_k + a = 0. \end{cases}$$

It is easy to conclude that when $a = \frac{(-1\pm\sqrt{b^2-bd+1})\left(2b^2-2bd+1\mp\sqrt{b^2-bd+1}\right)}{3b^2}$, there exists a fold bifurcation at the fixed point $E_k(x_k, y_k)$, where $x_k = \frac{-1\pm\sqrt{b^2-bd+1}}{b}$, $y_k = x_k - \frac{x_k^3}{3}$.

Next, the characteristic polynomial of the Jacobian matrix at the fixed point $E_k(x_k, y_k)$ of model (2) is

$$P(\lambda) = \lambda^2 + \left(\left(cx_k^2 - c + \frac{b}{c}\right)h - 2\right)\lambda + \left(bx_k^2 + 2x_k - b + d\right)h^2 - \left(cx_k^2 - c + \frac{b}{c}\right)h + 1.$$

Like the analysis of model (1), if the following conditions are satisfied, model (2) may undergo a fold bifurcation at the fixed point $E_k(x_k, y_k)$[24]:

$$\begin{cases} P(1)= \left(bx_k^2 + 2x_k - b + d\right) h^2 = 0, \\ \dfrac{b}{3}x_k^3 + x_k^2 + (d-b)x_k + a = 0. \end{cases}$$

It means that a fold bifurcation may occur at the fixed point $E_k(x_k, y_k)$ when $a = \frac{(-1\pm\sqrt{b^2-bd+1})\left(2b^2-2bd+1\mp\sqrt{b^2-bd+1}\right)}{3b^2}$, where $x_k = \frac{-1\pm\sqrt{b^2-bd+1}}{b}$, $y_k = x_k - \frac{x_k^3}{3}$.

For model (3), the characteristic polynomial corresponding to the Jacobian matrix at the fixed point $E_k(x_k, y_k)$ of model (3) is

$$h(\lambda) = \lambda^2 - p(a)\lambda + q(a),$$

where $p(a) = Ba + C, q(a) = Da + E$.

There exists a fold bifurcation at the fixed point $E_k(x_k, y_k)$ if the following conditions hold:

$$\begin{cases} h(1)=1 - p(a) + q(a)= 0 \\ \dfrac{b}{3}x_k^3 + x_k^2 + (d-b)x_k + a = 0 \end{cases}$$

Thus, when $a = a_0 = \frac{(-1\pm\sqrt{b^2-bd+1})\left(2b^2-2bd+1\mp\sqrt{b^2-bd+1}\right)}{3b^2}$, a fold bifurcation may occur at the fixed point $E_k(x_k, y_k)$, where $x_k = \frac{-1\pm\sqrt{b^2-bd+1}}{b}$, $y_k = x_k - \frac{x_k^3}{3}$.

It is easy to find that the conditions of the fold bifurcation for these three models are consistent.

Using the corresponding theorems in[24,25,26], we obtain the following result of model (3).

Theorem 3.1 If $\left|\frac{BE-CD+D}{B-D}\right| \neq 1$ and $\tilde{a}\left(a_0\right) \neq 0$, then model (3) undergoes a fold bifurcation at $E_k(x_k, y_k)$ when $a = a_0$. Moreover, if $\tilde{a}(a_0) < 0$ (resp., $\tilde{a}(a_0) > 0$), there are two fixed points for $a < a_0$ (resp., $a > a_0$). These two fixed points collide at $a = a_0$, and disappear when $a > a_0$ (resp., $a < a_0$).

Proof. The model (3) undergoes a fold bifurcation at the fixed point $E_k(x_k, y_k)$ as the parameter a varies in small neighborhood of a_0. There exists a critical eigenvalue $\lambda_1 = 1$. And supposing that $|\lambda_2| = \left|\frac{BE-CD+D}{B-D}\right| \neq 1, B - D \neq 0$ are satisfied. There exist $p_1, q_1 \in R^2$ such that $J(a_0, x_k, y_k)q_1 = q_1$ and $J^T(a_0, x_k, y_k)p_1 = p_1$, where $J^T(a_0, x_k, y_k)$ is the transpose matrix of $J(a_0, x_k, y_k)$.

It is easy to obtain

$$q_1 \sim (q_1^*, 1)^T,$$
$$p_1 \sim (p_1^*, 1)^T,$$

where

$$q_1^* = \frac{16(hc(bx_k^2+\frac{3}{2}(d-b)+3x_k)+3b)(hc^2(2x_k^2-3)+(6+(bx_k^2+\frac{3}{2}(d-b)+3x_k)h^2)c+3bh)(bx_k+\frac{3}{2})}{16(hc(bx_k^2+\frac{3}{2}(d-b)+3x_k)+3b)(hc^2(2x_k^2-3)+(6+(bx_k^2+\frac{3}{2}(d-b)+3x_k)h^2)c+3bh)(dx_k+\frac{1}{2}x_k^2+\frac{3}{2})},$$

$$p_1^* = \frac{-16(hc(bx_k^2+\frac{3}{2}(d-b)+3x_k)+3b)(hc^2(2x_k^2-3)+(6+(bx_k^2+\frac{3}{2}(d-b)+3x_k)h^2)c+3bh)(bx_k+\frac{3}{2})}{48c^2(bx_k+\frac{3}{2})(hc^2(2x_k^2-3)+(6+(bx_k^2+\frac{3}{2}(d-b)+3x_k)h^2)c+3bh)}.$$

For satisfying the normalization $< p_1, q_1 >= 1$, where $< p_1, q_1 >= p_1^*q_1^* + p_2^*q_2^* = p_1^*q_1^* + 1$ is the scalar product in R^2, we choose

$$q_1 = (q_1^*, 1)^T,$$
$$p_1 = \kappa_1(p_1^*, 1)^T,$$

where

$$\kappa_1 = \frac{1}{p_1^*q_1^* + 1}.$$

Through a series of transformations based on the theorems deduced by Kuznetsov[24], the restriction of the model (11) to its one-dimensional center manifold at the critical parameter values a_0 can be transformed into the normal form

$$\eta \mapsto \eta + \tilde{a}(a_0)\eta^2 + \tilde{b}(a_0)\eta^3 + O\left(\eta^4\right),$$

where

$$\tilde{a}\left(a_0\right) = \frac{1}{2}\langle p, B(q, q)\rangle,$$

$$\tilde{b}\left(a_0\right)=\frac{1}{6}\left(\langle p, C(q,q,q)\rangle-3\left\langle p, B\left(q,\left(A\left(a_0\right)-I_2\right)^{INV}a\right)\right\rangle\right),$$

$$a=B(q,q)-\langle p, B(q,q)\rangle q,$$

which determines the direction of fold bifurcation at the fixed point $E_k(x_k,y_k)$, where I_2 is the unit 2×2 matrix. In the fold case, the matrix $\left(A\left(a_0\right)-I_2\right)$ is noninvertible in R^2, since $\lambda_1=1$ is the eigenvalue of $A\left(a_0\right)$. Let T^{su} denotes an one dimensional linear eigenspace of $A\left(a_0\right)$ corresponding to all eigenvalues other than λ_1. Notice that $a\in T^{su}$, since $<$ p, $a>=0$. The restriction of the linear transformation corresponding to $A\left(a_0\right)$ to its invariant subspace T^{su} is invertible. Thus, in order to facilitate the following calculation, we use $\left(A\left(a_0\right)-I_2\right)^{INV}$ to denote the inverse of $\left(A\left(a_0\right)-I_2\right)$, where INV means the inverse in T^{su}. $[\left(A\left(a_0\right)-I_2\right)^{INV}a]$ can be computed by solving the following system

$$\begin{pmatrix} A-I_2 & q \\ p^T & 0 \end{pmatrix}\begin{pmatrix} \left(A\left(a_0\right)-I_2\right)^{INV}a \\ \eta \end{pmatrix}=\begin{pmatrix} a \\ 0 \end{pmatrix}$$

for $\left(A\left(a_0\right)-I_2\right)^{INV}a\in R^2$ and $\eta\in R^1$. Here q and p are the above-defined and normalized eigenvectors of $A\left(a_0\right)$ and $A^T(a_0)$, respectively. The 3×3 matrix of this system is nonsingular[24].

The proof is completed.

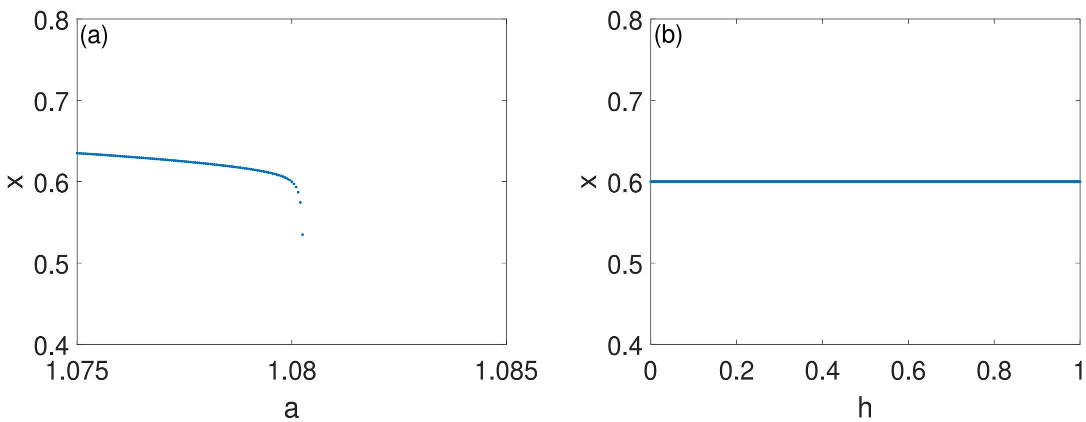

FIGURE 1 (a) Bifurcation diagram of model (3) in (a,x) plane for $b=5, c=1, d=2, h=0.1$, the initial condition is $(0.6, 0.528)$. (b) Bifurcation diagram of model (3) in (h,x) plane for $a=1.080, b=5, c=1, d=2$, the initial condition is $(0.6, 0.528)$.

3.2 | Neimark-Sacker bifurcation

As the fold bifurcation analysed above, a Neimark-Sacker bifurcation will be analysed in this section, the parameter a is chosen as the bifurcation parameter and bifurcation analysis is performed by bifurcation theory at the fixed point $E_k(x_k,y_k)$.

For model (1), if the following conditions are satisfied, a Neimark-Sacker bifurcation may occur at the fixed point $E_k(x_k,y_k)$:

$$\begin{cases} trace=(1-x^2)c^2-b=0, \\ \frac{b}{3}x^3+x^2+(d-b)x+a=0, \end{cases}$$

where the "trace" represents the trace of the Jacobian matrix of the model (1) at the fixed point $E_k(x_k,y_k)$.

It is easy to know from the above conditions that the model (1) may take place a Neimark-Sacker bifurcation at the fixed point $E_k(x_k,y_k)$ when

$a=a_1=\frac{\pm\left((2b-3d)c^2+b^2\right)\sqrt{c^2-b}-3c^3+3bc}{3c^3}$, where $x_k=\pm\frac{\sqrt{c^2-b}}{c}$, $y_k=x_k-\frac{x_k^3}{3}$.

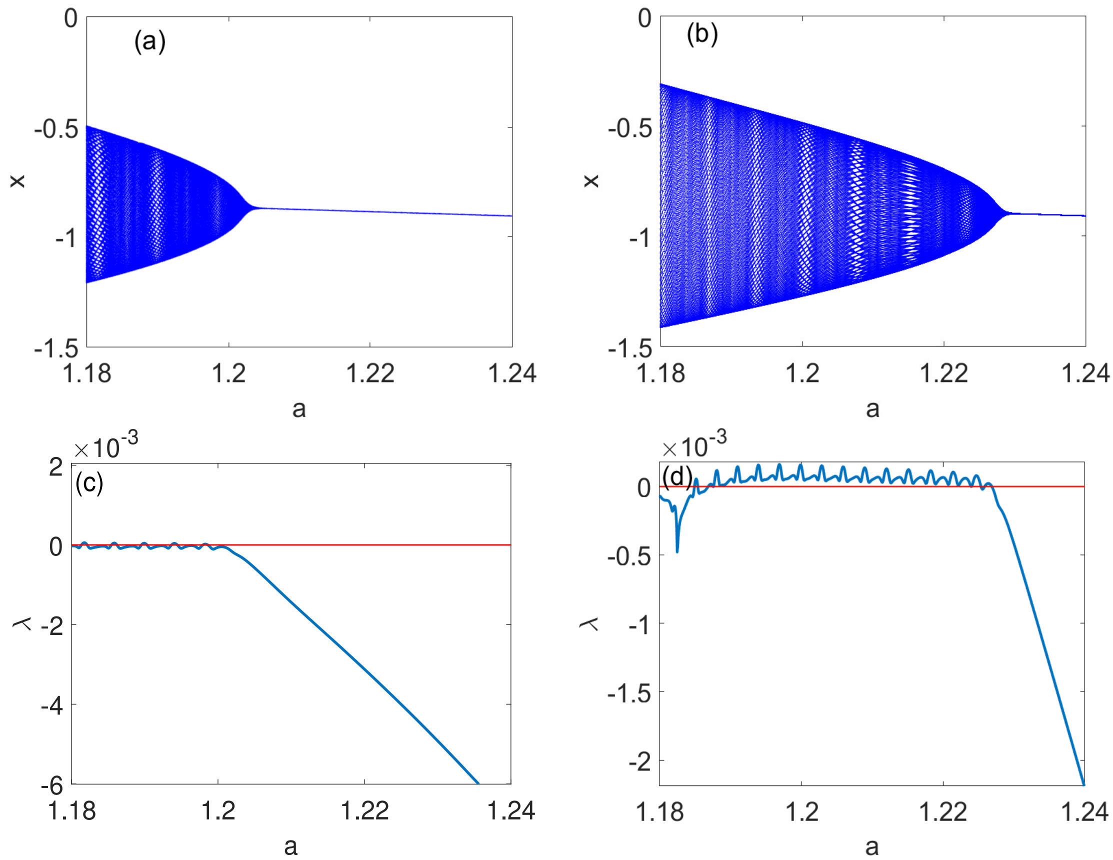

FIGURE 2 (a) Bifurcation diagram of model (3) in (a, x) plane for $b = 1, c = 2, d = 3, h = 0.1$, the initial condition is $(-0.8, -0.6)$. (b) Bifurcation diagram of model (2) in (a, x) plane for $b = 1, c = 2, d = 3, h = 0.1$, the initial condition is $(-0.8, -0.6)$. (c) Maximum Lyapunov exponents corresponding to (a). (d) Maximum Lyapunov exponents corresponding to (b).

Similarly, a Neimark-Sacker bifurcation may arise at the fixed point $E_k(x_k, y_k)$ of the model (2), if the following conditions hold:

$$\begin{cases} \left(1 - x_k^2\right) c^2 + \left(bx_k^2 - b + d + 2x_k\right) hc - b = 0, \\ \dfrac{b}{3} x_k^3 + x_k^2 + (d - b)x_k + a = 0. \end{cases}$$

Thus, when $a = a_2$, a Neimark-Sacker bifurcation may occur at the fixed point $E_k(x_k, y_k)$, where

$$\begin{aligned} a_2 = {} & \frac{(hc-\sqrt{(c^3-2h(b-\frac{d}{2})c^2+((b^2-bd+1)h^2-b)c+b^2h)c})}{3c^2(hb-c)^3} \\ & \times \frac{((3d-2b)c^3+(4b^2h-5bdh+3h)c^2+((2h^2d-1)b^2-2b^3h^2-bh^2-3\sqrt{(c^3-2h(b-\frac{d}{2})c^2+((b^2-bd+1)h^2-b)c+b^2h)c})c)}{3c^2(hb-c)^3} \\ & - \frac{bh(b^2+\sqrt{\left(c^3-2h\left(b-\frac{d}{2}\right)c^2+\left(\left(b^2-bd+1\right)h^2-b\right)c+b^2h\right)c})}{3c^2(hb-c)^3}, \end{aligned}$$

$$x_k = \frac{-hc \pm \sqrt{\left(c^3 - 2h\left(b - \frac{d}{2}\right)c^2 + \left(\left(b^2 - bd + 1\right)h^2 - b\right)c + b^2h\right)c}}{c(bh - c)}, y_k = x_k - \frac{x_k^3}{3}.$$

As the study of the model (1) and the model (2), a Neimark-Sacker bifurcation may undergo at the fixed point $E_k(x_k, y_k)$ of the model (3) if the following conditions are satisfied:

$$\begin{cases} q(a) = 1, \\ \dfrac{b}{3} x_k^3 + x_k^2 + (d - b)x_k + a = 0. \end{cases}$$

It means that when $a = a_3$, a Neimark-Sacker bifurcation may occur at the fixed point $E_k(x_k, y_k)$, where

$$a_3 = \pm \frac{\sqrt{6}\left((6d - 4b)c^2 + bh(b - d)c - 2b^2\right)\sqrt{c(bh - 6c)(b - c^2)} - 6c(bh - 6c)(b - c^2)}{c^2(bh - 6c)^2},$$

$$x_k = \pm \frac{\sqrt{6}\sqrt{c(bh-6c)\left(b-c^2\right)}}{c(bh-6c)}, y_k = x_k - \frac{x_k^3}{3}.$$

Since the relationship between a_1, a_2 and a_3 can not be directly seen through the above expressions, the specific comparison will be given in the later numerical simulation.

Using the corresponding results in[24,25,26], we obtain the following theorem.

Theorem 3.2 If the conditions $a \neq -\frac{C}{B}, -\frac{C-1}{B}$ hold and $\tilde{a}\left(a_3\right) \neq 0$, then model (3) undergoes a Neimark-Sacker bifurcation at $E_k(x_k, y_k)$ when $a = a_3$. Moreover, the sign of $\tilde{a}\left(a_3\right)$ decides the stability of bifurcating closed invariant curve. If $\tilde{a}\left(a_3\right) < 0$ (resp., $\tilde{a}\left(a_3\right) > 0$), then the bifurcating closed invariant curve is attracting (resp., repelling) for $a > a_3$ (resp., $a < a_3$).

Proof. The following characteristic equation is given to analysis the local dynamics near the fixed points of model (3):

$$\lambda^2 + p\left(a\right)\lambda + q\left(a\right) = 0,$$

where

$$p\left(a\right) = Ba + C,$$

$$q\left(a\right) = Da + E.$$

Then

$$|\lambda(a)| = \sqrt{Da + E},$$

$$l^* = \left.\frac{a|\lambda|}{da}\right|_{a=a_3} = \frac{D}{2} = \frac{24c^3h^3x_k - (12bx_k + 18)c^2h^4}{\left(ch^2\left(2bx_k^2 - 3b + 3d + 6x_k\right) + h\left(\left(4x_k^2 - 6\right)c^2 + 6b\right) + 12c\right)^2} \neq 0.$$

In addition, $\left|\lambda(a_3)\right| = 1$, and we require $p(a_3) \neq 0, 1$, which means

$$a_3 \neq -\frac{C}{B}, -\frac{C-1}{B}$$

then $\lambda^n(a_3) \neq 1$, $n = 1, 2, 3, 4$. There exist $p_3, q_3 \in C^2$ such that

$$A(a_3, x_k, y_k)q_3 = \lambda(a_3)q_3, A(a_3, x_k, y_k)\bar{q_3} = \bar{\lambda}(a_3)\bar{q_3}.$$

and

$$A^T(a_3, x_k, y_k)p_3 = \bar{\lambda}(a_3)p_3, A^T(a_3, x_k, y_k)\bar{p_3} = \lambda(a_3)\bar{p_3}.$$

After calculation, p,q can be chosen as

$$q_3 \sim (q_3^*, 1)^T,$$

$$p_3 \sim (p_3^*, 1)^T,$$

where

$$\begin{aligned} q_3^* = & \frac{-\frac{1}{2}c((bhx_k-2cx_k)+\frac{3}{2}h)\sqrt{2}\sqrt{128}}{\left(ch^2\left(2bx_k^2-3b+3d+6x_k\right)+h\left(\left(4x_k^2-6\right)c^2+6b\right)+12c\right)^2} \\ & \times \frac{\sqrt{c(hc^2(2x_k^2-3)+(6+(bx_k^2+\frac{3(d-b)}{2}+3x_k)h^2)c+3bh)^2(h(x_k^3-\frac{3x_k}{2})c^2+(\frac{3h^2x_k^2}{8}+3x_k)c-\frac{9h}{4})}}{\left(ch^2\left(2bx_k^2-3b+3d+6x_k\right)+h\left(\left(4x_k^2-6\right)c^2+6b\right)+12c\right)^2(2bhx_k-4cx_k+3h)^2} \\ & \times \frac{\sqrt{(\frac{9-3x_k^2-6dx_k}{2})c^2+hc(bx_k^2+\frac{3(d-b)}{2}+3x_k)(bx_k+\frac{3}{2})+3b^2x_k+\frac{9b}{2}}}{\left(ch^2\left(2bx_k^2-3b+3d+6x_k\right)+h\left(\left(4x_k^2-6\right)c^2+6b\right)+12c\right)^2(2bhx_k-4cx_k+3h)^2} \\ & + \frac{4c\left(h\left(2x_k^2-3\right)c^2+\left(6+\left(bx_k^2-\frac{3}{2}b+\frac{3}{2}d+3x_k\right)h^2\right)c+3bh\right)c\left(h\left(bx_k^3-\frac{3}{2}bx_k+\frac{9}{4}x_k^2-\frac{9}{4}\right)c+3bx_k\right)}{\left(ch^2\left(2bx_k^2-3b+3d+6x_k\right)+h\left(\left(4x_k^2-6\right)c^2+6b\right)+12c\right)^2}, \end{aligned}$$

$$\begin{aligned} p_3^* = & \frac{2\sqrt{2}(bhx_k-2cx_k+\frac{3}{2}h)\sqrt{128}}{24\left(-2cx_k+h\left(bx_k+\frac{3}{2}\right)\right)\left(h\left(2x_k^2-3\right)c^2+\left(6+\left(bx_k^2-\frac{3}{2}b+\frac{3}{2}d+3x_k\right)h^2\right)c+3bh\right)c^2} \\ & \times \frac{\sqrt{c(hc^2(2x_k^2-3)+(6+(bx_k^2+\frac{3(d-b)}{2}+3x_k)h^2)c+3bh)^2(h(x_k^3-\frac{3x_k}{2})c^2+(\frac{3h^2x_k^2}{8}+3x_k)c-\frac{9h}{4})}}{\left(24\left(-2cx_k+h\left(bx_k+\frac{3}{2}\right)\right)\left(h\left(2x_k^2-3\right)c^2+\left(6+\left(bx_k^2-\frac{3}{2}b+\frac{3}{2}d+3x_k\right)h^2\right)c+3bh\right)c^2\right)(2bhx_k-4cx_k+3h)^2} \\ & \times \frac{(\frac{9-3x_k^2-6dx_k}{2})c^2+hc(bx_k^2+\frac{3(d-b)}{2}+3x_k)(bx_k+\frac{3}{2})+3b^2x_k+\frac{9b}{2}}{\left(24\left(-2cx_k+h\left(bx_k+\frac{3}{2}\right)\right)\left(h\left(2x_k^2-3\right)c^2+\left(6+\left(bx_k^2-\frac{3}{2}b+\frac{3}{2}d+3x_k\right)h^2\right)c+3bh\right)c^2\right)(2bhx_k-4cx_k+3h)^2} \\ & + \frac{16\left(h\left(2x_k^2-3\right)c^2+\left(6+\left(bx_k^2-\frac{3}{2}b+\frac{3}{2}d+3x_k\right)h^2\right)c+3bh\right)c\left(h\left(bx_k^3-\frac{3}{2}bx_k+\frac{9}{4}x_k^2-\frac{9}{4}\right)c+3bx_k\right)}{24\left(-2cx_k+h\left(bx_k+\frac{3}{2}\right)\right)\left(h\left(2x_k^2-3\right)c^2+\left(6+\left(bx_k^2-\frac{3}{2}b+\frac{3}{2}d+3x_k\right)h^2\right)c+3bh\right)c^2}. \end{aligned}$$

Normalizing p_3 with respect to q_3, we have

$$q_3 = (q_3^*, 1)^T,$$

$$p_3 = \kappa_3(p_3^*, 1)^T,$$

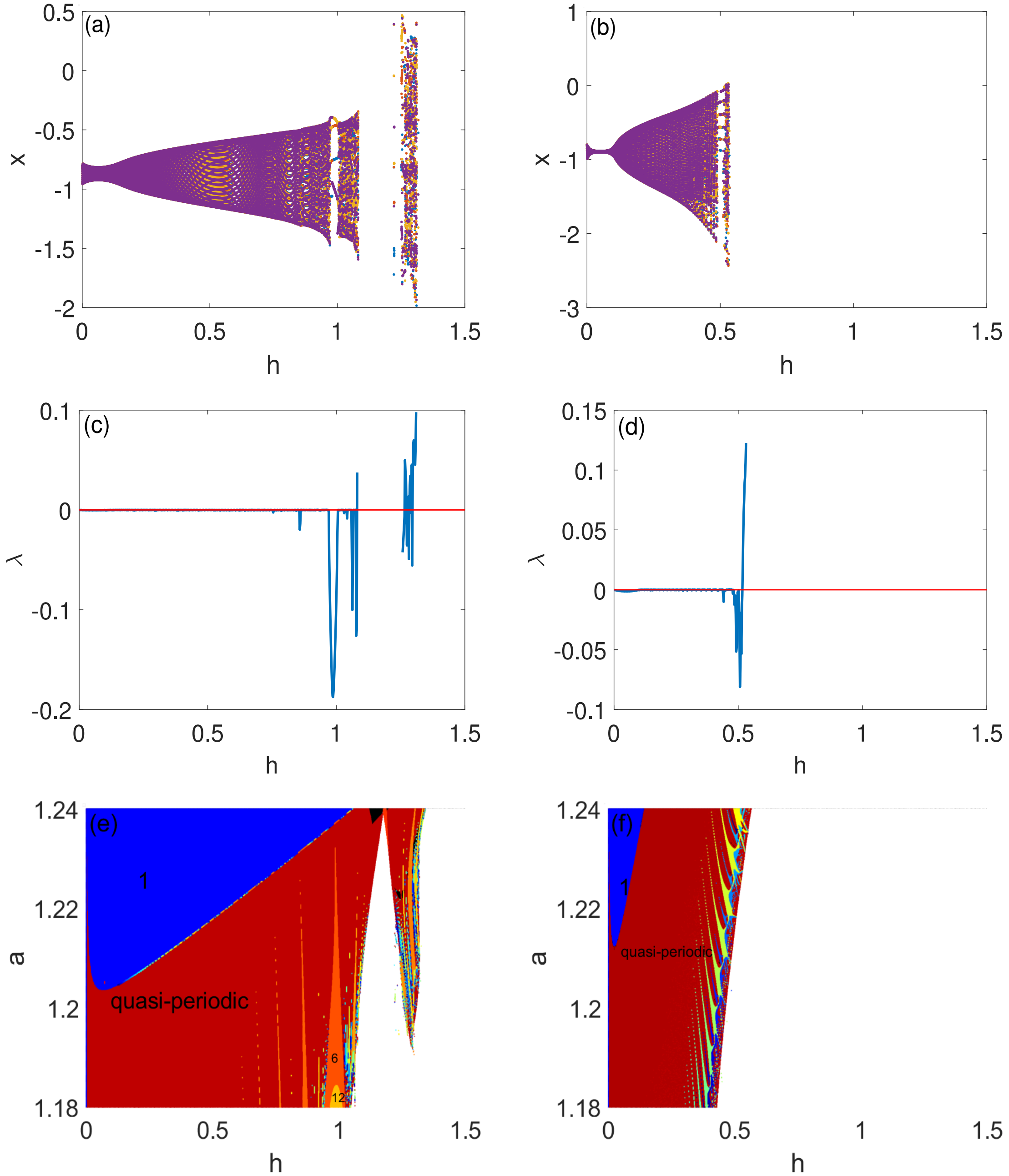

FIGURE 3 (a) Bifurcation diagram of model (3) in (h, x) plane for $a = 1.2023, b = 1, c = 2, d = 3$, the initial condition is $(-0.8, -0.6)$. (b) Bifurcation diagram of model (2) in (h, x) plane for $a = 1.2277, b = 1, c = 2, d = 3$, the initial condition is $(-0.8, -0.6)$. (c) Maximum Lyapunov exponents corresponding to (a). (d) Maximum Lyapunov exponents corresponding to (b). (e) Two-dimensional parameter-plane diagram in (h, a) plane corresponding to (a). (f) Two-dimensional parameter-plane diagram in (h, a) plane corresponding to (b).

where

$$\kappa_3 = \frac{1}{p_3^* q_3^* + 1}.$$

Through the transformations based on the theorems [24], the restriction of the model (11) to the center manifold takes the form

$$z \mapsto e^{i\theta(a_3)} z(1 + \tilde{d}\left(a_3\right)|z|^2) + O(|z|^4),$$

where $e^{i\theta(a_3)} = \lambda\left(a_3\right), z \in Z^2$ and the real number $\tilde{d}\left(a_3\right) = \mathrm{Re}\left(d\left(a_3\right)\right)$ is given by the following formula:

$$\begin{aligned}\tilde{d}\left(a_3\right) = \frac{1}{2}\mathrm{Re}\Big\{ e^{-i\theta(a_3)}\Big[\langle p, C(q,q,\bar{q})\rangle + 2\Big\langle p, B\Big(q, \left(I_2 - A\left(a_3\right)\right)^{-1} B(q,\bar{q})\Big)\Big\rangle \\ + \Big\langle p, B\Big(\bar{q}, \left(e^{2i\theta(a_3)} I_2 - A\left(a_3\right)\right)^{-1} B(q,q)\Big)\Big\rangle\Big]\Big\}.\end{aligned}$$

The proof is completed.

4 | NUMERICAL SIMULATIONS

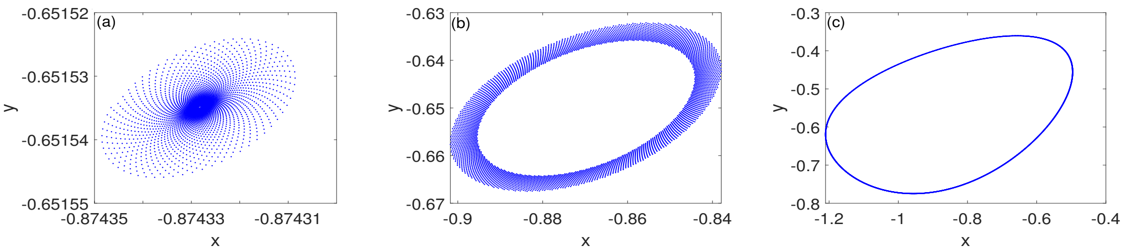

FIGURE 4 Phase portraits for various values of h corresponding to Fig. 2(a). (a) Orbits for $a = 1.207$. (b) Orbits for $a = 1.20235$. (c) An invariant cycle for $a = 1.18$.

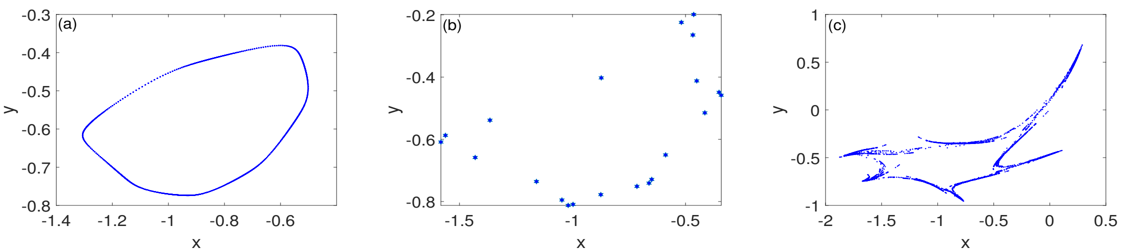

FIGURE 5 Phase portraits for various values of h corresponding to Fig. 3(a). (a) An invariant cycle for $h = 0.855$. (b) Period-21 orbits for $h = 1.081$. (c) A chaotic attractor for $h = 1.299$, and the corresponding Maximum Lyapunov exponents is about equal to 0.06967.

In the following cases, we consider different bifurcation parameters respectively. Case (i) chooses the parameter a and the step size h as the bifurcation parameter respectively. Case (ii) choose a as the free parameter. In order to compare the NSFD scheme with the forward Euler scheme, the step size h is chosen as the free parameter to carry out bifurcation analysis of model (2) and model (3) respectively in case (iii).

(i) When $a = 1.080$, $b = 5$, $c = 1$, $d = 2$ and $h = 0.1$, Seen from Fig. 1(a), model (3) undergoes the fold bifurcation at the point $(0.6, 0.528)$ with $\tilde{a}(a_0) = -0.5127203730 < 0$. So two fixed points bifurcated from $(0.6, 0.528)$ for $a < a_0$ which is illustrated by Theorem 3.1. Fig. 1(b) presents bifurcation diagram which shows the bifurcating process for $h \in (0, 1)$ and confirms that fold bifurcation is independent of the value of h.

(ii) When $a = 1.202251732$, $b = 1$, $c = 2$, $d = 3$ and $h = 0.1$, there exists a unique fixed point $(-0.8696565516, -0.6504154051)$ for model (3). When $a \approx 1.202251732$, the Neimark-Sacker bifurcation occurs at the point $(-0.8696565516, -0.6504154051)$ and its eigenvalues are $\lambda_{1,2} \approx 0.9947971165 \pm 0.1018758902i$. For $a = 1.202251732$, there are $|\lambda| = 1$, $l^* = \dfrac{d\,|\lambda|}{d a_3} = -0.0006179753 < 0$ and $\tilde{d}(a_3) = -3.476537096 < 0$. Fixed parameters $h = 0.1$, $b = 1$, $c = 2$, $d = 3$, model (2) undergoes the Neimark-Sacker bifurcation at $(-0.8947368423, -0.6559751179)$ when

$a \approx 1.227681392$. It is easy to compute that model (1) undergoes the Hopf bifurcation at $(-0.8660254043, -0.6495190530)$ when $a \approx 1.198557159$. The error of bifurcation parameter a of model (3) is $e_1 = |a_3 - a_1| = 0.003694573$, while the error of model (2) is $e_2 = |a_2 - a_1| = 0.029124233 > 0.003694573$. So we conclude that the Neimark-Sacker bifurcation of model (3) is closer to model (1) than model (2). Fig. 2(a) presents the bifurcation diagrams which show the process of bifurcation and the occurrence of a closed invariant curve. Fig. 2(b) corresponds to the forward Euler method. We also plot the maximum Lyapunov exponents which show the emergence of periodic orbits and chaotic region when the free parameter a changes in Figs. 2(c)-(d). Some typical phase portraits of model (3) are also plotted in Fig. 4.

(iii) Corresponding to the conditions (ii), the step size h is chosen as the bifurcation parameter. Figs. 3(a)-(b) display the bifurcation diagrams which show the bifurcating process of the Neimark-Sacker bifurcation of model (3) and model (2), respectively. The stability of the fixed points is illustrated by calculating the maximum Lyapunov exponents in Figs. 3(c)-(d) respectively corresponding to Figs. 3(a)-(b). In order to have a more intuitive comparison between the NSFD scheme and the forward Euler scheme, two-dimensional parameter-plane diagrams of model (2) and model (3) are presented respectively in Fig. 3(e) and Fig. 3(f), which show the emergence of the chaotic phenomenon and periodic structure clearly. Comparing Fig. 3(e) with Fig. 3(f), within the same range, Fig. 3(f) has more overflow, which is due to the divergence of the forward Euler scheme. So we infer that applying the NSFD scheme to discretize a continuous-time system could get more results. Moreover, we can see more complex dynamic phenomena. As we see in Fig. 3(a), the fixed point undergoes the Neimark-Sacker bifurcation and enclosed by a closed invariant cycle. When the step size h lies in a small neighborhood of 1.2299, the corresponding maximum Lyapunov exponents are positive, which implies the possibility of the occurrence of the chaotic phenomena[27]. The occurrence of closed invariant curves and chaotic attractors are displayed in Fig. 5.

Meanwhile, the variation between $e_1 = |a_3 - a_1|$ and the step size h is given in Table 1, which demonstrates that the Hopf bifurcation of the model (3) which obtained by the NSFD method is more closer to the original model (model (1)) than the model (2) which obtained by the forward Euler method. Furthermore, since model (1) is independent of h so that a_0 is taken as $a_0 = 1.198557159$ in Table 1. From Table 1, it is obviously clear that as $h \to 0$, the critical values of bifurcation parameter a for emergence of Hopf bifurcation and Neimark-Sacker bifurcation are nearly identical, that is, $e_1 = |a_3 - a_1| \to 0$.

5 | CONCLUSIONS

In this paper, a discrete-time Hindmarsh-Rose model is obtained by the NSFD scheme in R^2. Fortunately, it's explicit expression can be solved, which facilitates our research. The fold bifurcation and the Neimark-Sacker bifurcation have been investigated by using the center manifold theorem and bifurcation theory.

Compared with the forward Euler scheme, our investigation demonstrates that the difference equation obtained by the NSFD scheme is closer to the original continuous system. The convergency and stability of the NSFD scheme is much better than the forward Euler scheme, which has been demonstrated by comparing the relevant properties between model (2) and model (3). When the step size h increases, the forward Euler method diverges earlier than the NSFD method, which makes the model (3) that obtained by the NSFD method get more dynamic behavior. Moreover, taking the Hopf bifurcation as an example, when the step

TABLE 1 Variation of a_3 and $|a_3 - a_1|$ with different values of h.

h	a_3	$\|a_3 - a_1\|$
0.0000001	1.198557163	4×10^{-9}
0.00001	1.198557526	3.67×10^{-7}
0.001	1.198593893	0.000036734
0.1	1.202251732	0.003694573
0.3	1.209771941	0.011214782
0.5	1.217473491	0.018916332
0.7	1.225364787	0.026807628
0.7577854710	1.227681393	$0.029124234 \approx e_2$

size h is the same, bifurcation parameter of model (3) is closer to the original continuous model than model (2). Therefore, it is much more better to use the NSFD scheme to discretize continuous systems than the forward Euler scheme from the perspective of retaining the structure of the original system as much as possible.

Due to the complexity of this Hindmarsh-Rose model, it is hard to obtain the direct relationship of the eigenvalues of the Jacobian matrices between the differential equations and the resulting difference equations by a strict theoretical way. So it limits the strict theoretical deduction concerning the comparison between the differential equations and the resulting difference equations in depth. Therefore, what we can do depends on mostly the bifurcation analysis and numerical simulations, respectively. Even so, it is worthwhile to take into account these comparison between the NSFD scheme and the forward Euler scheme. This is because through these comparisons, on the one hand, we can build up much more experience to deal with the similar problem. On the other hand, these confirmed methods can guarantee to obtain true numerical results for complex neuron dynamical systems.

ACKNOWLEDGMENTS

This work is supported by the State Key Laboratory of Traction Power, Southwest Jiaotong University under Project No. TPL2001 and the Infrastructure Inspection Research Institute, China Academy of Railway Science under Project No. S18L00250.

Conflict of interest

The authors declare no potential conflict of interests.

References

1. Mickens RE. Nonstandard Finite Difference Models of Differential Equations. *World Sci.* 1993.
2. Bairagi N, Biswas M. A predator-prey model with Beddington-DeAngelis functional response: a non-standard finite-difference method. *J. Differ. Equ. Appl.* 2015;1-13.
3. Dimitrov DT, Kojouharov HV. Nonstandard finite-difference methods for predator-prey models with general functional response. *Math. Comput. Simulat.* 2008;78:1-11.
4. Moghadas SM, Alexander ME, Corbett BD. A non-standard numerical scheme for a generalized Gause-type predator-prey model. *Physica D.* 2004;188:134-151.
5. Roeger LIW. Nonstandard finite-difference schemes for the Lotka-Volterra systems: generalization of Mickens's method. *J. Differ. Equ. Appl.* 2006;12:937-948.
6. Roeger LIW, Lahodny G. Dynamically consistent discrete Lotka-Volterra competition systems. *J. Differ. Equ. Appl.* 2013;19:191-200.
7. Kahan W. Li RC. Unconventional Schemes for a Class of Ordinary Differential Equations-With Applications to the Korteweg-de Vries Equation. *J. Comput. Physics.* 1997;134:316-331.
8. Roeger LIW. Local Stability of Euler's and Kahan's Methods. *J. Differ. Equ. Appl.* 2004;10:601-614.
9. Castro MÁ, Sirvent A, Rodríguez F. Nonstandard finite difference schemes for general linear delay differential systems. *Math Meth Appl Sci.* 2020;1-15.
10. Namjoo M, Zeinadini M, Zibaei S. Nonstandard finite-difference scheme to approximate the generalized Burgers-Fisher equation. *Math Meth Appl Sci.* 2018;41:821-8228.
11. Geng Y, Xu J. Stability preserving NSFD scheme for a multi-group SVIR epidemic model. *Math. Meth. Appl. Sci.* 2017;40:4917-4927.

12. Wang Y. Dynamics of a nonstandard finite-difference scheme for delay differential equations with unimodal feedback. *Commun. Nonlinear Sci. Numer. Simulat.* 2012;17:3967-3978.

13. Wang H, Zheng Y, Lu Q. Stability and bifurcation analysis in the coupled HR neurons with delayed synaptic connection. *Nonlinear Dyn.* 2017;88:1-10.

14. Yu Y, Cao H. Integral step size makes a difference to bifurcations of a discrete-time Hindmarsh-Rose model. *Int. J. Bifurcation and Chaos* 2015;25:1550029.

15. Li B, He Z. Bifurcations and chaos in a two-dimensional discrete Hindmarsh-Rose model. *Nonlinear Dyn.* 2013;76.

16. Felicio CC, Rech PC. Arnold tongues and the Devil's staircase in a discrete-time Hindmarsh-Rose neuron model. *Phys. Lett. A* 2015;379:2845-2847.

17. Kuznetsov AP. Sedova YV. The simplest map with three-frequency quasi-periodicity and quasi-periodic bifurcations. *Int. J. Bifurcation and Chaos* 2016;26:1630019.

18. Umer S, Irfan A. Qamar D. Neimark-Sacker bifurcation and chaos control in discrete-time predator-prey model with parasites. *Nonlinear Dyn.* 2018.

19. Singh H, Dhar J, Bhatti H. Discrete-time bifurcation behavior of a prey-predator system with generalized predator. *Advances in Differ. Equ.* 2015;2015:1-15.

20. Cheng L, Cao H. Bifurcation analysis of a discrete-time ratio-dependent predator-prey model with Allee effect. *Commun. Nonlinear Sci. Numer. Simulat.* 2016;38:288-302.

21. Jiang XW, Zhan XS, Jiang B. Stability and Neimark-Sacker bifurcation analysis for a discrete single genetic negative feedback autoregulatory system with delay. *Nonlinear Dyn.* 2014;76:1031-1039.

22. Tsuji S, Ueta T, Kawakami H, Fujii H, Aihara K. Bifurcations in two-dimensional Hindmarsh-Rose type model. *Int. J. Bifurcation and Chaos* 2007;17:985-998.

23. Li B, He Q. Bifurcation analysis of a two-dimensional discrete Hindmarsh-Rose type model. *Advances in Differ. Equ.* 2019;2019:124.

24. Kuznetsov YA. Elements of applied bifurcation theory. *Appl. Math. Sci.* 2004;288:715-730.

25. Wiggins S. Introduction to applied nonlinear dynamical systems and chaos. *Springer*. 1990.

26. Guckenheimer J, Holmes P. Nonlinear oscillations, dynamical systems, and bifurcations of vector fields. *Springer*. 1983.

27. Edward O. Chaos in dynamical systems. *Cambridge University Press*. 2002.

APPENDIX

$$
\begin{aligned}
J_{11} = {} & \frac{-24\left(x_k{}^2-4x_k y_k+\frac{3}{2}\right)h^2c^4+48h\left(\left(\left(-\frac{1}{2}x_k{}^2+x_k y_k-\frac{3}{4}\right)b+\frac{dx_k{}^2}{4}+ax_k+\frac{3d}{4}+\frac{3y_k}{2}\right)h^2-x_k{}^2\right)c^3}{4\left(h\left(2x_k{}^2-3\right)c^2+\left(6+\left(bx_k{}^2-\frac{3}{2}b+\frac{3}{2}d+3x_k\right)h^2\right)c+3bh\right)^2} \\
& + \frac{\left(144+\left(\left(-6x_k{}^2\ -9\right)b^2+\left(6dx_k{}^2+24ax_k+18d\right)b-9d^2+36a\right)h^4-48bh^2x_k{}^2\right)c^2}{4\left(h\left(2x_k{}^2-3\right)c^2+\left(6+\left(bx_k{}^2-\frac{3}{2}b+\frac{3}{2}d+3x_k\right)h^2\right)c+3bh\right)^2} \\
& + \frac{\left(-12b^2h^3x_k{}^2+144bh\right)c+36b^2h^2}{4\left(h\left(2x_k{}^2-3\right)c^2+\left(6+\left(bx_k{}^2-\frac{3}{2}b+\frac{3}{2}d+3x_k\right)h^2\right)c+3bh\right)^2},
\end{aligned}
$$

$$
J_{12} = \frac{-12c^2h}{h\left(4x_k{}^2-6\right)c^2+\left(\left(2bx_k{}^2-3b+3d+6x_k\right)h^2+12\right)c+6bh},
$$

$$
\begin{aligned}
J_{21} = {} & \frac{6\left(c^2\left(\frac{bdx_k{}^4}{6}+dx_k{}^3+a+\frac{3}{2}-\frac{3}{4}db\right)x_k{}^2+\left(\left(a+\frac{3}{2}\right)d-\frac{3b}{2}\right)x_k+\frac{3a}{2}\right)h^3}{\left(c\left(bx_k{}^2-\frac{3}{2}b+\frac{3}{2}d+3x_k\right)h^2+\left(\left(2x_k{}^2-3\right)c^2+3b\right)h+6c\right)^2} \\
& -\frac{3ch^2\left(\left(-\frac{dx_k{}^4}{9}+\left(\frac{d}{2}-\frac{2y_k}{3}\right)x_k{}^2+\left(1-\frac{2dy_k}{3}\right)x_k-y_k\right)c^2-\left(\frac{db}{6}+1\right)x_k{}^2-dx_k+\frac{db}{2}-\frac{d^2}{2}+a\right)}{\left(c\left(bx_k{}^2-\frac{3}{2}b+\frac{3}{2}d+3x_k\right)h^2+\left(\left(2x_k{}^2-3\right)c^2+3b\right)h+6c\right)^2} \\
& +\frac{\left(\left(dx_k{}^2-3d-6y_k\right)c^2+3b(d+2x_k)\right)h+6c(d+2x_k))h}{\left(c\left(bx_k{}^2-\frac{3}{2}b+\frac{3}{2}d+3x_k\right)h^2+\left(\left(2x_k{}^2-3\right)c^2+3b\right)h+6c\right)^2},
\end{aligned}
$$

$$
J_{22} = \frac{h\left(4x_k{}^2-6\right)c^2+\left(12-\left(2bx_k{}^2-3b+3d+6x_k\right)h^2\right)c-6bh}{h\left(4x_k{}^2-6\right)c^2+\left(12+\left(2bx_k{}^2-3b+3d+6x_k\right)h^2\right)c+6bh},
$$

$$
B = \frac{(24bx_k+36)c^2h^4+48c^3x_kh^3}{4\left(c\left(bx_k{}^2-\frac{3}{2}b+\frac{3}{2}d+3x_k\right)h^2+\left(\left(2x_k{}^2-3\right)c^2+3b\right)h+6c\right)^2},
$$

$$
\begin{aligned}
C = {} & \frac{-c^2h^4\left(b^2x_k^4+6bx_k^3+\left(-\frac{3}{2}b^2+9+\frac{3}{2}bd\right)x_k^2+9(d-b)x_k+\frac{9(b-d)^2}{2}\right)}{\left(\left(2x_k^2-3\right)hc^2+\left(6+\left(bx_k^2-\frac{3}{2}b+\frac{3}{2}d+3x_k\right)h^2\right)c+3bh\right)^2} \\
& -\frac{ch^3\left(\left((6b-3d)x_k^2-12bx_ky_k+9b-9d-18y_k\right)c^2+9b\left(bx_k^2-b+d+2x_k\right)\right)}{\left(\left(2x_k^2-3\right)hc^2+\left(6+\left(bx_k^2-\frac{3}{2}b+\frac{3}{2}d+3x_k\right)h^2\right)c+3bh\right)^2} \\
& -\frac{12\left(\left(-\frac{1}{3}x_k^3+\frac{3}{2}x_k-2y_k\right)c^2+bx_k\right)x_kc^2h^2+\left(\left(36-12x^2\right)c^2-36b\right)ch-72c^2}{\left(\left(2x^2-3\right)hc^2+\left(6+\left(bx^2-\frac{3}{2}b+\frac{3}{2}d+3x_k\right)h^2\right)c+3bh\right)^2},
\end{aligned}
$$

$$
D = \frac{48c^3x_kh^3-(24bx_k+36)c^2h^4}{4\left(c\left(bx_k{}^2+\frac{3}{2}(d-b)+3x_k\right)h^2+\left(\left(2x_k{}^2-3\right)c^2+3b\right)h+6c\right)^2},
$$

$$
E = \frac{-24\left(x_k^2-4x_ky_k+\frac{3}{2}\right)h^2c^4-48\left(\left(-\frac{3dx_k^2}{4}+\left(by_k-\frac{3}{2}\right)x_k+\frac{3y_k}{2}\right)h^2+x_k^2\right)hc^3}{4\left(\left(2x_k^2-3\right)hc^2+\left(6+\left(bx_k^2+\frac{3}{2}(d-b)+3x_k\right)h^2\right)c+3bh\right)^2}.
$$

$$
\begin{aligned}
b_1 = {} & -\frac{2\left(6hc^2+\left((3b-3d)h^2+12\right)c+6bh\right)\left(-8hc^2x_k+(-4bx_k+6)h^2c\right)}{\left(4h\left(-\frac{3}{2}+x_k{}^2\right)c^2+\left(12+\left(2bx_k{}^2-3b+3d-6x_k\right)h^2\right)c+6bh\right)^2} \\
& -\frac{\left(6h(-x_k+2y_k)c^2+\left(((3d-3b)x_k-6a)h^2-12x_k\right)c-6bhx_k\right)\left(4bch^2+8hc^2\right)}{\left(4h\left(-\frac{3}{2}+x_k{}^2\right)c^2+\left(12+\left(2bx_k{}^2-3b+3d-6x_k\right)h^2\right)c+6bh\right)^2} \\
& +\frac{2\left(6h(-x_k+2y_k)c^2+\left(((3d-3b)x_k-6a)h^2-12x_k\right)c-6bhx_k\right)\left(-8hc^2x_k+(-4bx_k+6)h^2c\right)^2}{\left(4h\left(-\frac{3}{2}+x_k{}^2\right)c^2+\left(12+\left(2bx_k{}^2-3b+3d-6x_k\right)h^2\right)c+6bh\right)^3},
\end{aligned}
$$

$$
\begin{aligned}
b_2 = {} & \frac{4c(by_k-3dx_k+2a+3)h^2+\left(-8c^2y_k+24\right)h}{c\left(2bx_k{}^2-3b+3d-6x_k\right)h^2+\left(\left(4x_k{}^2-6\right)c^2+6b\right)h+12c} \\
& -\frac{(8c(\frac{3(y_k+dx_k^2)}{2}-2x_k(a+\frac{by_k+3}{2}))h^2+8(2c^2x_ky_k+3d-6x_k)h)((6-4bx_k)h^2c-8hx_kc^2)}{\left(c\left(2bx_k{}^2-3b+3d-6x_k\right)h^2+\left(\left(4x_k{}^2-6\right)c^2+6b\right)h+12c\right)^2} \\
& +\frac{2(ch^2(4x_k^2(a+\frac{by_k+3}{2})-6(x_ky_k+a)-dx_k^3-3y_k(b-a))+(12(a+x_k^2)+c^2y_k(6-4x_k^2)+6by_k-12dx_k)h-12cy_k)}{\left(c\left(2bx_k^2-3b+3d-6x_k\right)h^2+\left(\left(4x_k^2-6\right)c^2+6b\right)h+12c\right)^2} \\
& \times\frac{((6-4bx_k)h^2c-8hx_kc^2)^2}{\left(c\left(2bx_k{}^2-3b+3d-6x_k\right)h^2+\left(\left(4x_k{}^2-6\right)c^2+6b\right)h+12c\right)^3} \\
& -\frac{(ch^2(4x_k^2(a+\frac{by_k+3}{2})-6(x_ky_k+a)-dx_k^3-3y_k(b-a))+(12(a+x_k^2)+c^2y_k(6-4x_k^2)+6by_k-12dx_k)h-12cy_k)}{\left(c\left(2bx_k^2-3b+3d-6x_k\right)h^2+\left(\left(4x_k^2-6\right)c^2+6b\right)h+12c\right)^2} \\
& \times\frac{4(bch^2+2hc^2)}{\left(c\left(2bx_k^2-3b+3d-6x_k\right)h^2+\left(\left(4x_k^2-6\right)c^2+6b\right)h+12c\right)^2},
\end{aligned}
$$

$$
b_3 = \frac{12hc^2\left(-8hx_kc^2+(-4bx_k+6)h^2c\right)}{\left(4h\left(-\frac{3}{2}+x_k{}^2\right)c^2+\left(12+\left(2bx_k{}^2-3b+3d-6x_k\right)h^2\right)c+6bh\right)^2},
$$

$$
\begin{aligned}
b_4 = {} & \frac{4(ch^2(bx_k-\frac{3}{2})-2hx_kc^2)}{c\left(2bx_k^2-3b+3d-6x_k\right)h^2+\left(\left(4x_k^2-6\right)c^2+6b\right)h+12c} \\
& -\frac{\left(ch^2(6x_k-2bx_k^2+3(b-d))+((4x_k{}^2-6)c^2-6b)h+12c\right)((6-4bx_k)h^2c-8hx_kc^2)}{\left(c\left(2bx_k^2-3b+3d-6x_k\right)h^2+\left(\left(4x_k^2-6\right)c^2+6b\right)h+12c\right)^2},
\end{aligned}
$$

$$
\begin{aligned}
c_1 = {} & \frac{6(6hc^2+((3b-3d)h^2+12)c+6bh)((6-4bx_k)h^2c-8hx_kc^2)^2}{(4hc^2(x_k{}^2-\frac{3}{2})+(12+(2bx_k{}^2-3b+3d-6x_k)h^2)c+6bh)^3} \\
& -\frac{12(6hc^2+((3b-3d)h^2+12)c+6bh)(bch^2+2hc^2)}{(4hc^2(x_k{}^2-\frac{3}{2})+(12+(2bx_k{}^2-3b+3d-6x_k)h^2)c+6bh)^2} \\
& -\frac{6\left(6h(-x_k+2y_k)c^2+\left(((3d-3b)x_k-6a)h^2-12x_k\right)c-6bhx_k\right)\left(-8hxc^2+(-4bx_k+6)h^2c\right)^3}{\left(4h\left(-\frac{3}{2}+x_k{}^2\right)c^2+\left(12+\left(2bx_k{}^2-3b+3d-6x_k\right)h^2\right)c+6bh\right)^4} \\
& -\frac{6\left(6h(-x_k+2y_k)c^2+\left(((3d-3b)x_k-6a)h^2-12x_k\right)c-6bhx_k\right)\left(-8hc^2x_k+(-4bx_k+6)h^2c\right)\left(4bch^2+8hc^2\right)}{\left(4h\left(-\frac{3}{2}+x_k{}^2\right)c^2+\left(12+\left(2bx_k{}^2-3b+3d-6x_k\right)h^2\right)c+6bh\right)^3},
\end{aligned}
$$

$$
\begin{aligned}
c_2 = &\frac{12cdh^2}{ch^2(2bx_k{}^2-3b+3d-6x_k)+((4x_k{}^2-6)c^2+6b)h+12c}\\
&-\frac{3(4c(by_k-3dx_k+2a+3)h^2+(24-8c^2y_k)h)((6-4bx_k)h^2c-8hx_kc^2)}{(ch^2(2bx_k{}^2-3b+3d-6x_k)+((4x_k{}^2-6)c^2+6b)h+12c)^2}\\
&+\frac{6\left(4c\left(-2x_k\left(a+\frac{by_k}{2}+\frac{3}{2}\right)+\frac{3y_k}{2}+\frac{3dx_k{}^2}{2}\right)h^2+\left(8c^2x_ky_k+12d-24x_k\right)h\right)\left(-8hc^2x_k+(-4bx_k+6)h^2c\right)^2}{\left(c\left(2bx_k{}^2-3b+3d-6x_k\right)h^2+\left(\left(4x_k{}^2-6\right)c^2+6b\right)h+12c\right)^3}\\
&-\frac{3\left(4c\left(-2x_k\left(a+\frac{by_k}{2}+\frac{3}{2}\right)+\frac{3y_k}{2}+\frac{3dx_k{}^2}{2}\right)h^2+\left(8c^2x_ky_k+12d-24x_k\right)h\right)\left(4bch^2+8hc^2\right)}{\left(c\left(2bx_k{}^2-3b+3d-6x_k\right)h^2+\left(\left(4x_k{}^2-6\right)c^2+6b\right)h+12c\right)^2}\\
&-\frac{6(4ch^2(x_k{}^2(a+\frac{by_k+3}{2})-\frac{3(x_ky_k+a+dx_k{}^3)}{2}-\frac{3y_k(b-1)}{4})+(12(a+x^2)+c^2(6y-4x^2y)+6by-12xd)h-12cy)}{\left(c\left(2bx^2-3b+3d-6x\right)h^2+\left(\left(4x_kx^2-6\right)c^2+6b\right)h+12c\right)^4}\\
&\times\frac{((6-4bx)h^2c-8hxc^2)^3}{\left(c\left(2bx^2-3b+3d-6x\right)h^2+\left(\left(4x_kx^2-6\right)c^2+6b\right)h+12c\right)^4}\\
&+\frac{6(4ch^2(x_k^2(a+\frac{by_k+3}{2})-\frac{3(x_ky_k+a+dx_k^3)}{2}-\frac{3y_k(b-1)}{4})+(12(a+x_k^2)+c^2y_k(6-4x_k^2)+6by_k-12dx_k)h-12cy_k)}{\left(c\left(2bx_k^2-3b+3d-6x_k\right)h^2+\left(\left(4x_k^2-6\right)c^2+6b\right)h+12c\right)^3}\\
&\times\frac{((6-4bx_k)h^2c-8hx_kc^2)(4bch^2+8hc^2)}{\left(c\left(2bx_k^2-3b+3d-6x_k\right)h^2+\left(\left(4x_k^2-6\right)c^2+6b\right)h+12c\right)^3},
\end{aligned}
$$

$$
\begin{aligned}
c_3 = &-\frac{24hc^2\left(-8hx_kc^2+(-4bx_k+6)h^2c\right)^2}{\left(4h\left(-\frac{3}{2}+x_k{}^2\right)c^2+\left(12+\left(2bx_k{}^2-3b+3d-6x_k\right)h^2\right)c+6bh\right)^3}\\
&+\frac{12hc^2\left(4bch^2+8hc^2\right)}{\left(4h\left(-\frac{3}{2}+x_k{}^2\right)c^2+\left(12+\left(2bx_k{}^2-3b+3d-6x_k\right)h^2\right)c+6bh\right)^2},
\end{aligned}
$$

$$
\begin{aligned}
c_4 = &\frac{4(-bch^2+2hc^2)}{ch^2(2bx_k{}^2-3b+3d-6x_k)+((4x_k{}^2-6)c^2+6b)h+12c}\\
&-\frac{2(4ch^2(bx_k-\frac{3}{2})-8hx_kc^2)((6-4bx_k)h^2c-8hx_kc^2)}{(ch^2(2bx_k{}^2-3b+3d-6x_k)+((4x_k{}^2-6)c^2+6b)h+12c)^2}\\
&+\frac{2\left(4c\left(-\frac{1}{2}bx_k{}^2+\frac{3}{2}x_k+\frac{3}{4}b-\frac{3}{4}d\right)h^2+\left(\left(4x_k{}^2-6\right)c^2-6b\right)h+12c\right)\left(-8hx_kc^2+(-4bx_k+6)h^2c\right)^2}{\left(c\left(2bx_k{}^2-3b+3d-6x_k\right)h^2+\left(\left(4x_k{}^2-6\right)c^2+6b\right)h+12c\right)^3}\\
&-\frac{\left(4c\left(-\frac{1}{2}bx_k{}^2+\frac{3}{2}x_k+\frac{3}{4}b-\frac{3}{4}d\right)h^2+\left(\left(4x_k{}^2-6\right)c^2-6b\right)h+12c\right)\left(4bch^2+8hc^2\right)}{\left(c\left(2bx_k{}^2-3b+3d-6x_k\right)h^2+\left(\left(4x_k{}^2-6\right)c^2+6b\right)h+12c\right)^2}.
\end{aligned}
$$

The proof of Theorem 2.1 and Theorem 2.2 is as follow:

1. $\Delta < 0$:

When $\Delta < 0$, that is $\frac{-BC+2D-2\sqrt{B^2E-BCD+D^2}}{B^2} < a < \frac{-BC+2D+2\sqrt{B^2E-BCD+D^2}}{B^2}$, then there exist two pairs of conjugate complex eigenvalues of model (3) as follows:

$$
\lambda_{1,2} = \frac{1}{2}\left(Ba+C \pm i\sqrt{4(Da+E)-(Ba+C)^2}\right).
$$

The modules of these eigenvalues at the fixed point E_k are easily calculated and found to be $\left|\lambda_{1,2}\right| = \sqrt{Da+E}$. Next, the following two cases should be considered.

Case 1: The fixed point E_k is a stable focus if $\left|\lambda_{1,2}\right| < 1$, i.e., the following conditions are satisfied:

$$
\left\{\begin{array}{c}\Delta < 0,\\ \left|\lambda_{1,2}\right| < 1.\end{array}\right. \Rightarrow \left\{\begin{array}{c}\frac{-BC+2D-2\sqrt{B^2E-BCD+D^2}}{B^2} < a < \frac{-BC+2D+2\sqrt{B^2E-BCD+D^2}}{B^2},\\ a < \frac{1-E}{D}(D>0); a > \frac{1-E}{D}(D<0).\end{array}\right. \tag{13}
$$

From the inequalities (13), we obtain
$\frac{-BC+2D-2\sqrt{B^2E-BCD+D^2}}{B^2} < a < \frac{-BC+2D+2\sqrt{B^2E-BCD+D^2}}{B^2}$, $a < \frac{1-E}{D}(D>0)$
or $\frac{-BC+2D-2\sqrt{B^2E-BCD+D^2}}{B^2} < a < \frac{-BC+2D+2\sqrt{B^2E-BCD+D^2}}{B^2}$, $a > \frac{1-E}{D}(D<0)$.

Case 2: The fixed point E_k is an unstable focus if $\left|\lambda_{1,2}\right| > 1$, i.e., the following conditions are satisfied:

$$
\left\{\begin{array}{c}\Delta < 0,\\ \left|\lambda_{1,2}\right| > 1.\end{array}\right. \Rightarrow \left\{\begin{array}{c}\frac{-BC+2D-2\sqrt{B^2E-BCD+D^2}}{B^2} < a < \frac{-BC+2D+2\sqrt{B^2E-BCD+D^2}}{B^2},\\ a > \frac{1-E}{D}(D>0); a < \frac{1-E}{D}(D<0).\end{array}\right. \tag{14}
$$

From the inequalities (14), we obtain
$\frac{-BC+2D-2\sqrt{B^2E-BCD+D^2}}{B^2} < a < \frac{-BC+2D+2\sqrt{B^2E-BCD+D^2}}{B^2}$, $a > \frac{1-E}{D}(D>0)$
or $\frac{-BC+2D-2\sqrt{B^2E-BCD+D^2}}{B^2} < a < \frac{-BC+2D+2\sqrt{B^2E-BCD+D^2}}{B^2}$, $a < \frac{1-E}{D}(D<0)$.

2. $\Delta \geq 0$:

When $\Delta \geq 0$, that is $a \geq \frac{2D-BC+2\sqrt{B^2E-BCD+D^2}}{B^2}$ or $a \leq \frac{2D-BC-2\sqrt{B^2E-BCD+D^2}}{B^2}$, then there exist two different real eigenvalues of model (3) as follows:

$$\lambda_{1,2} = \frac{1}{2}\left(Ba + C \pm \sqrt{(Ba+C)^2 - 4(Da+E)}\right).$$

There are three cases depending on the modules of $|\lambda_{1,2}|$.

Case 1: The fixed point E_k is a stable sink if $|\lambda_{1,2}| < 1$, i.e., the following conditions are satisfied:

$$\begin{cases} \Delta \geq 0, \\ h(1) > 0, \\ h(-1) > 0, \\ -2 < \lambda_1 + \lambda_2 < 2, \\ -1 < \lambda_1\lambda_2 < 1. \end{cases} \Rightarrow \begin{cases} a \geq \frac{2D-BC+2\sqrt{B^2E-BCD+D^2}}{B^2} \text{or} a \leq \frac{2D-BC-2\sqrt{B^2E-BCD+D^2}}{B^2}, \\ a < \frac{1+E-C}{B-D}(B-D>0); a > \frac{1+E-C}{B-D}(B-D<0), \\ a < \frac{-1-E-C}{B+D}(B+D<0); a > \frac{-1-E-C}{B+D}(B+D>0), \\ \frac{-C-2}{B} < a < \frac{-C+2}{B}(B>0); \frac{-C+2}{B} < a < \frac{-C-2}{B}(B<0), \\ -1 < Da + E < 1. \end{cases} \tag{15}$$

It is easy to calculate that there is no solution to the inequalities (15).

Case 2: The fixed point E_k is an unstable source if $|\lambda_{1,2}| > 1$, i.e., the following conditions are satisfied:

$$\begin{cases} \Delta \geq 0, \\ h(1) > 0, \\ h(-1) < 0. \end{cases} \Rightarrow \begin{cases} a \geq \frac{2D-BC+2\sqrt{B^2E-BCD+D^2}}{B^2} \text{or} a \leq \frac{2D-BC-2\sqrt{B^2E-BCD+D^2}}{B^2}, \\ a < \frac{1+E-C}{B-D}(B-D<0); a > \frac{1+E-C}{B-D}(B-D>0), \\ a < \frac{-1-E-C}{B+D}(B+D>0); a > \frac{-1-E-C}{B+D}(B+D<0). \end{cases} \tag{16}$$

or

$$\begin{cases} \Delta \geq 0, \\ \frac{Ba+C}{2} < -1, \\ h(-1) > 0. \end{cases} \Rightarrow \begin{cases} a \geq \frac{2D-BC+2\sqrt{B^2E-BCD+D^2}}{B^2} \text{or} a \leq \frac{2D-BC-2\sqrt{B^2E-BCD+D^2}}{B^2}, \\ a < -\frac{C+2}{B}(B>0); a > -\frac{C+2}{B}(B<0), \\ a < \frac{-1-E-C}{B+D}(B+D<0); a > \frac{-1-E-C}{B+D}(B+D>0). \end{cases} \tag{17}$$

or

$$\begin{cases} \Delta \geq 0, \\ \frac{Ba+C}{2} > 1, \\ h(1) > 0. \end{cases} \Rightarrow \begin{cases} a \geq \frac{2D-BC+2\sqrt{B^2E-BCD+D^2}}{B^2} \text{or} a \leq \frac{2D-BC-2\sqrt{B^2E-BCD+D^2}}{B^2}, \\ a > \frac{-C+2}{B}(B>0); a > \frac{-C+2}{B}(B<0), \\ a < \frac{1+E-C}{B-D}(B-D>0); a > \frac{1+E-C}{B-D}(B-D<0). \end{cases} \tag{18}$$

Case 3: The fixed point E_k is a saddle if $|\lambda_1| < 1, |\lambda_2| > 1$, or $|\lambda_1| > 1, |\lambda_2| < 1$, i.e., the following conditions are satisfied:

$$\begin{cases} \Delta > 0, \\ h(-1)h(1) < 0. \end{cases} \Rightarrow \begin{cases} a \geq \frac{2D-BC+2\sqrt{B^2E-BCD+D^2}}{B^2} \text{or} a \leq \frac{2D-BC-2\sqrt{B^2E-BCD+D^2}}{B^2}, \\ a \in R, D^2 - B^2 < 0. \end{cases} \tag{19}$$

From the inequalities (19), we obtain
$a \geq \frac{2D-BC+2\sqrt{B^2E-BCD+D^2}}{B^2}$
or $a \leq \frac{2D-BC-2\sqrt{B^2E-BCD+D^2}}{B^2}(D^2 - B^2 < 0)$.

□